Influence of cracking on the durability of lightweight aggregate structural concrete versus normal weight aggregate concrete

Bruno de Melo Felisberto

Department of Civil Engineering, Architecture and Georesources, Instituto Superior Técnico, Universidade de Lisboa

Abstract

This paper aims to evaluate the influence of cracking on the durability of structural lightweight aggregate concrete (SLWAC) and its behavior compared to normal weight aggregate concrete (NWAC). This study involves an extensive experimental campaign, which comprises mechanical and durability characterization tests. For this study, two types of lightweight aggregate with different porosities (Stalite and Leca) and pastes of different compactness were considered. Concretes were previously subjected to the induction of natural (mechanical tests) or artificial cracks ("Notch method"). The obtained results allow to conclude that, except for the chloride migration, the influence of artificial cracks on durability was not significantly affected by the type of aggregate. For concrete subjected to natural cracking, there was a greater participation of more porous aggregates, leading to a higher cracking influence on LWAC durability. For carbonation and chloride penetration, a linear relationship between the diffusion properties and crack opening was found, considering artificial cracks with apertures between 0,1 and 0,3 mm.

1. Introduction

Concrete is a quasi-brittle material that is highly susceptible to cracking during its designed service life. Cracks in concrete can develop for different reasons. Mechanical actions and poor designing can induce structural cracks while hygrothermal variations, differential settlements, restrained shrinkage and concrete deterioration mechanisms, such as freezing and thawing, and other expansive reactions can lead to non-structural cracking [1]. Basically, when the local tensile stresses in concrete exceed its maximum tensile strength, cracks are formed, and new external and internal paths are established [2]. These new paths should increase concrete permeability and may favour the penetration of deleterious species, inevitably affecting its durability.

Various studies have been conducted regarding the influence of cracks on the transport properties of conventional NWAC [2–11]. Studies focused on the permeability of cracked concrete have shown converging results. Earlier studies, such as those by Wang et al. [4] and Aldea et al. [7], using feedback-controlled splitting tensile tests concluded that crack widths lower than 0.05 mm had little influence on concrete water permeability. Within a range that varied from 0.05 mm to about 0.1-0.2 mm [3, 4], permeability steeply increased with crack width. Beyond the upper bound of this range permeability also increased, but steadily, with increasing crack width. Yang et al. [11] studied the influence of mechanically and freeze-thaw induced cracks on concrete sorptivity. The former crack inducing method created discreetly distributed cracks that influenced local water absorption, but not the overall sorptivity. The freeze-thaw action led to a linear increase of sorptivity, due to the higher connectivity and more uniform distribution of the crack pattern. Zhang et al. [8] concluded that the presence of cracks on the concrete surface, even the finest microcracks, are immediately filled with water as soon as the cracked surface is put into contact with water.

To achieve comparable results several authors have established critical crack widths to quantify the effects of this parameter on deterioration mechanisms of corrosion induced by carbonation and chloride attack [5, 6, 9, 10]. The critical crack width serves as a threshold value from which point, a further increase in the crack opening has no significant influence on the diffusion rate, at least no more than the one accountable to surface effects under uncracked conditions. Djerbi et al. [6] studied the influence of mechanically induced cracks with 0.2-0.7 mm widths on the chloride diffusion coefficient. The diffusion coefficient increased linearly with increasing crack width up to 0.08 mm. Further increase of crack width had little effect on the chloride diffusion coefficient. Similar conclusions were obtained by Jang et al. [10], who also reported 0.05-0.08 mm for the threshold crack width in chloride diffusion of cracked concrete.

Green-Sullivan [5] described the relationship between crack width and carbonation depth as an "S" shaped curve, i.e. a lower bound connected to an upper bound by a transitioning curve. For small crack openings (< 0.5 mm) there was no significant increase in the measured property. Over 0.5 mm, the carbonation rate increased linearly with increasing crack width up to a threshold value. After this limit, the carbonation rate stabilized, and diffusion was no

longer influenced by further increasing crack width. According to the author, in this upper range differences in carbonation rate should be mainly dominated by other effects, such as surface conditions, internal humidity and lower permeability, due to carbonation products that are eventually formed.

With the increasing use of lightweight aggregate concrete (LWAC), research on this material has intensified in recent decades [12-17, 20]. Nonetheless, there is still lack of knowledge on LWAC behaviour, especially regarding its durability and the main mechanisms governing its deterioration. Although some studies have focused on the transport properties and deterioration mechanisms of cracked NWC and uncracked LWAC, to the best of the author's knowledge no studies on the performance of LWAC under cracked conditions have been put forward. In this context, this paper aims to study the influence of cracking on the capillary absorption, oxygen permeability, carbonation resistance and chloride penetration resistance of LWAC. For this purpose, the effects of inducing artificial and natural cracks on LWAC produced with different types of aggregate and water/cement ratios (w/c) is analysed, as well as its relative performance when compared to cracked NWAC.

2. Experimental program

2.1 Materials

The experimental campaign involved the production of several LWAC with differen tw/c, 0.35 and 0.55. For the production of the admixtures, two types of LWA were used: Leca (expanded clay aggregate) and Stalite (expanded slate aggregate), which physical properties are presented in Table 1. Normal weight aggregates (NWA) consisted on crushed limestone composed by coarse gravel 1 (CG1), coarse gravel 2 (CG2) and fine gravel (FG), and natural silica sand, composed of fine sand (FS) and coarse sand (CS)(Table 1). In addition, cement type I 42.5R, and, a superplasticizer were also used to produce these mixtures.

Table 1: Aggregate properties

Property	Normal weight aggregates					Lightweight aggregates	
	Fine sand	Coarse sand	Fine gravel	Coarse gravel 1	Coarse gravel 2	Leca	Stalite
24h water absorption, $w_{abs,24h}$ (%)	0.19	0.26	0.73	0.35	1.05	16.28	3.57
Particle dry density, ρ_p (kg/m^3)	2605	2617	2646	2683	2618	969	1483
Loose bulk density, ρ_b (kg/m^3)	1569	1708	1309	1346	1325	632	760
Shape index	-	-	34 (SI_{40})	20 (SI_{20})	15 (SI_{15})	1 (SI_{15})	10 (SI_{15})

2.2 Mixture composition and production

For the formulation of the mixtures, the Faury method was adopted, following the methodology proposed by Bogas [20], in order to take into account, the specificity of LWAC, particularly with regard to the fact that its workability, endurance and density are conditioned by the type and volume of aggregate. In Table 2, the compositions of the various mixtures considered for the development of this experimental campaign are summarized. The mixtures were formulated for different w/c, to encompass distinct compactness pastes, representative of the most usual range of LWAC. For each type of aggregate, it was sought to ensure that the mixtures presented the same w/c and paste volume, in order to make the analysis of the influence of the type of aggregate possible for concretes of equal composition.

The concrete was produced in a vertical axis mixer. First, the aggregates were introduced in the mixer and then moistened for 3 minutes with 1/3 of the mixing water. The absorption of LWA was estimated according to the method suggested by Bogas & Gomes [26]. Then, the cement, the remaining water and, when needed, the superplasticizer, were added to the mixture. The final mixture time was about 7 minutes in mixtures with w/c of 0.35, 0,6% of cement weight of superplasticizer was used.

The concrete production for the physical characterization (28 days) consisted of three 150 mm cubic specimens (for compressive strength) and two 100 mm cubic specimens (for concrete dry density), for the different mixtures produced. Concerning the durability, eight ϕ150x300 mm cylindrical specimens (for capillary absorption and oxygen

permeability), twenty-four ϕ100x200 mm cylindrical specimens and three 600x150x150 mm prisms (for carbonation resistance and chloride-ion penetration resistance), for the different mixtures produced.

Table 2: Mix proportions

Aggregate	Binder	w/c	Cement content (kg/m^3)	Paste vol. (L/m^3)	Volume of Coarse aggregate (L/m^3)	Volume of Natural sand (L/m^3)		Volume of Water (L/m^3)
						Fine	Coarse	
NWA	CEM I	0.35	450	330	435	80	154	158
Stalite					355	100	214	
Leca					355	114	201	
NWA		0.55	350	330	402	114	154	193
Stalite					355	114	201	
Leca					355	134	181	

2.3 Curing process

The demoulding process took place 24 hours after the concrete production. The specimens used for compressive strength and concrete dry density tests were water cured until the age of testing. The specimens for the capillary absorption and oxygen permeability tests were water cured for 7 days, followed by 7 days in a controlled chamber at 22 ± 2 ºC with 50 ± 5% relative humidity (RH); then oven dried for 3 days at 60 °C; plus 10 days at 60 °C involved in cellophane and 1 day at testing room temperature. The specimens used for carbonation resistance and chloride penetration tests were water cured for 7 days, then placed in a controlled chamber at a temperature of 22 ± 2 °C and 50 ± 5% RH until testing.

2.4 Crack formation

In order to study the transport properties of cracked concrete, cracks have to be generated in a concrete specimen. There are two main groups of cracks that can be induced in concrete specimens: artificial and natural cracks. Artificial cracks present a major disadvantage, which is that they do not exactly reflect reality, the surface of the notches contains more cement than the surface of a real crack and they are not tortuous. However, artificial cracks are easy to model and have clear results. The main advantage of natural cracks is that they can reproduce reality. However, it is very complicated to model the experimental results and ensure the required aperture.

Concrete specimens were made with artificial cracks by means of the positioning and removal of thin brass sheets inside the specimen, after approximately 4 or 5 h, depending on the w/c. These brass sheets had a thickness of 0.1, 0.2 and 0.3 mm. The sheets were inserted in the specimen 20 mm deep. This depth was chosen so that the final specimen, after the necessary cuts, had a crack of the desired thickness and a depth of about 10 mm. This method of artificial pre-cracking was implemented in the plastic molds that served as a basis for the production of the specimens used in the carbonation resistance, chloride penetration, capillarity and permeability to oxygen tests.

The natural cracks were created by a three-point bending test, on reinforced concrete prisms with 150 x 150 x 600 mm. The loading was conducted uniformly with a velocity of 0.002 mm/s or 0. 005 mm/s, depending on whether it was a NWAC or LWAC specimen, respectively. Next, three concrete ϕ95 x 150 mm cores were drilled from the reinforced concrete prism, containing the cracks. After that, these concrete cores were sectioned in order to obtain specimens 50 mm high, to carry out the carbonation resistance and chloride penetration tests.

2.5 Tests methods

2.5.1 Capillary absorption

Capillary absorption was determined at 28 days in compliance with specification E393 [21]. The test consists in measuring the water uptake of a concrete specimen in contact with a 5 mm film of water. A rate of water absorption was obtained by measuring the mass increase of the samples over time. Mass measurements were taken 10, 20, 30, 60 minutes and 3, 6, 24 and 72 hours after the initial contact with water. The absorption coefficient was obtained through the slope of the linear regression line between √20 min and √60 min of each tested specimen and then averaged. For

each mixture 6 specimens were tested, three with a 0.3 mm artificial crack and three non-cracked specimens, all ϕ 150 x 50 mm.

2.5.2 Oxygen permeability

The oxygen permeability tests were conducted according to the specification E392 [22], based on the Cembureau method. The equipment consisted in three permeability cells (where specimens were placed and subjected to lateral pressure), an oxygen supply cylinder, a permeameter from Testing company and a stop-watch. The coefficient of permeability was obtained using Eq. (1) of Hagen-Poiseuille at constant pressure for compressible fluids, where Kg is the permeability coefficient (m^2); η is the coefficient of viscosity of the gas ($N.s/m^2$); Q is the gas flow (m^3); l is the thickness of the specimen (m); A is the cross-sectional area (m^2); p is the atmospheric pressure (N/m^2); p_1 is the input pressure (N/m^2); p_2 is the output pressure (N/m^2); and t is the time (s). For each mixture 6 specimens were tested, 3 with a 0.3 mm artificial crack and 3 non-cracked specimens, all ϕ 150 x 50 mm.

2.5.3 Carbonation resistance

The accelerated carbonation test was done according to the specification E391 [23]. The specimens were kept in a carbonation chamber at 23 ± 3 ºC, 60 ± 5% RH and 3 ± 0,1% of CO_2. The carbonation depth was measured after spraying a phenolphthalein solution on the freshly broken surfaces. A carbonation coefficient can be obtained from the carbonation depth by applying Fick's first law of diffusion trough Eq. (2), where x_c is the measured carbonation depth and K_c the carbonation coefficient. For the analysis of the carbonation resistance in specimens with artificial cracks (0, 0.1, 0.2 and 0.3 mm), the specimens were subjected to accelerated carbonation for 28, 56 and 91 days. For each mixture and age, 2 specimens were tested. For the analysis of the carbonation resistance in specimens with natural cracks, specimens were subjected to accelerated carbonation during 7 and 28 days, in this case only mixtures with a w/c of 0.55 were tested. For each mixture, 3 specimens were tested.

2.5.4 Chloride penetration resistance

The chloride penetration resistance was determined according to the specification E463 [24], based on NTbuild492 [25], which provides a chloride ion migration diffusion coefficient (D_{cl}) under non-steady conditions. The migration coefficient was calculated according to Eq. (3), where T represents the average value of the initial and final temperature of the anodic solution (ºC), L is the specimen's thickness (mm), U is the absolute value of the applied voltage (V), t is the test duration (hours) and x_d is the average value of the measured chloride penetration depth (mm). For the analysis of chloride penetration resistance in specimens with artificial cracks, 3 specimens were tested for each composition and cracking type. For a w/c of 0.35, were considered non-cracked specimens and specimens with cracks apertures of 0.1; 0.2 and 0.3 mm. For mixtures with a w/c of 0.55, cracks with 0.2 mm of aperture were not considered. This test was also applied to specimens with natural cracks, for mixtures with w/c of 0.35 and 0.55.

$$K_g = \eta \frac{Q\,L}{t\,A} \frac{2p}{(p_1^2 - p_2^2)} \qquad \text{(Eq.1)}$$

$$x_c = K_c t^{0,5}\ [mm/year^{0,5}] \qquad \text{(Eq.2)}$$

$$Dcl = \frac{0{,}0239(273+T)L}{(U-2)t}\left(x_d - 0{,}0238\sqrt{\frac{(273+T)Lx_d}{U-2}}\right)\ [\mathrm{x}10^{-12}\ m^2/\mathrm{s}] \qquad \text{(Eq.3)}$$

3. Results and discussion

3.1 Compressive strength and dry density

Table 3 lists the fresh and dry densities (ρf and ρd), the compressive strength, (fc,28d), the structural efficiency (fc,28d/ρd) and the slump measurements, for each composition. The results suggest that Stalite is oriented to produce high strength concrete, while Leca is better suited to produce medium to low strength concrete. Naturally, NWAC reported higher compressive strength results compared to LWAC, for identical mixtures. However, it should be stated

that the highest structural efficiency was produced using LWA (Stalite). As expected, the structural efficiency tends to decrease with the increase of w/c.

Table 3: Fresh and dry densities, the compressive strength, the structural efficiency and the slump measurements

Aggregate	Binder	w/c	ρ_f (kg/m^3)	ρ_d (kg/m^3)	$f_{c,28d}$ (MPa)	$f_{c,28d}/\rho_d$ (x10^3 m)	Slump (cm)
NWA	CEM I	0.35	2420	2341	74.7	31.9	13
		0.55	2337	2270	51.2	22.6	10
Stalite		0.35	2006	1881	61.6	32.7	16
		0.55	1948	1802	41.2	22.8	13
Leca		0.35	1909	1702	35.1	20.6	14
		0.55	1861	1622	26.8	16.5	11

3.2 Capillary absorption

The results presented in Table 4 include water absorptions at different times (Abs.), capillary absorption coefficients (C_{abs}) values, relative humidity (RH) values and medium crack length (L_c). Th capillary absorption coefficients varied between 52,3 and 197,9 x10^{-6} m/min^{0,5}, which places the analyzed concretes on the scale proposed by Browne [19], between medium and high quality.

Table 4: Results of Capillary absorption tests

		Non-cracked specimens					Cracked specimens					
Aggregate	w/c	Abs. (kg/m^2)			C_{abs} (x10^{-6} m/min^{0,5})	RH (%)	Abs. (kg/m^2)			C_{abs} (x10^{-6} m/min^{0,5})	RH (%)	L_c (mm)
		10 min	6 h	72 h			10 min	6 h	72 h			
NWA	0.35	0.27	1.16	2.47	52.3	63.7	0.36	1.43	2.78	64.2	53.8	9.0
	0.55	0.45	2.94	4.66	149.8	60.0	0.60	3.04	4.64	148.8	59.1	9.8
Stalite	0.35	0.32	1.51	3.13	72.4	54.9	0.45	1.74	3.5	77.0	56.7	15.5
	0.55	0.64	3.57	5.50	183.8	53.2	0.78	3.73	5.37	186.3	52.9	14.9
Leca	0.35	0.39	1.44	2.93	62.9	70.4	0.53	1.64	3.19	66.5	61.8	16.2
	0.55	0.75	3.83	6.58	188.7	58.8	0.91	4.16	6.75	197.9	62.1	14.0

3.2.1 Capillary absorption in non-cracked concrete

Analyzing the results of non-cracked specimens, it is possible to verify that, for the same w/c, the different types of concrete have results of the same order of magnitude. However, the absorption over time and the absorption rate tend to be slightly higher in the concrete with more porous aggregates. Although capillary absorption is essentially governed by the w/c, it is verified that it is also affected by the type of aggregate. Contrary to what was observed by other authors [15,20], the absorption coefficient was higher in LWAC than in NWAC. This was due to the fact that the specimens used in this study were drier than those used by the authors mentioned above, leading to a greater participation by the aggregates in capillary absorption.

3.2.2 Capillary absorption in cracked concrete

As expected, cracked specimens tend to exhibit higher absorption and absorption coefficients over non-cracked reference specimens, however the differences were not very significant. Due to difficulties of execution, it was not possible to guarantee the same L_c for all cracked specimens. Thus, the absorption coefficients of the different types of concrete cannot be directly compared. In order to quantify the influence of the presence of cracks in concrete and allow a comparison between different types of concrete, a crack influence coefficient (K_{cl}) was defined, according to Eq. (4), where $Abs_{cracked}$ and $Abs_{non\text{-}cracked}$ represent the water absorptions at 6 h (mm/min$^{0.5}$) of the cracked and the non-cracked specimens, respectively, A_0 the area (mm^2) of the specimen in contact with water and *D* the specimen diameter (mm).

$$k_{CI} = \frac{\frac{\mathrm{Abs}_{\,cracked}\ \mathrm{x}\ \mathrm{A_0}}{\mathrm{A_0} + (2\ \mathrm{L}_c\ \mathrm{x}\ \mathrm{D})}}{\mathrm{Abs}_{\,\mathrm{non-cracked}}} \qquad \text{(Eq.4)}$$

Table 5: Coefficient K_{CI} values

Aggregate	w/c	K_{CI}
NWA	0.35	1.099
	0.55	0.886
Stalite	0.35	0.913
	0.55	0.834
Leca	0.35	0.890
	0.55	0.878

From the analysis of the K_{CI} values, it is possible to verify that the greater the compactness of the paste, the greater the influence of the crack. This influence tends to be slightly higher in the NWAC than in the LWAC. A greater increase of absorption by the LWAC in comparison to the NWAC, due to the presence of artificial cracking with aperture of 0.3 mm, is not confirmed. For a better understanding of the influence of a crack in concrete specimens, the absorption coefficients of the crack area ($C_{abs,CA}$) were calculated according to Eq. (5) and Eq. (6). The term $C_{abs,CA}$ (x 10^{-6} m/min^{0,5}) represents the additional mass of water that has been absorbed by the cracked specimen, due to the existence of a crack. A_c represents the crack surface area (mm^2), given by the multiplication of the crack aperture, w_c (mm), by the diameter of the specimen, D. Table 6 shows the values of $C_{abs,CA}$ for the initial moments of water absorption (10min). These results indicate that the absorption coefficients of the crack area were about 2 to 3 orders of magnitude higher than in non-cracked concrete.

$$C\ abs_{CA} = \frac{Abs_{CA}}{W_c\ x\ D\ x\ \sqrt{t}} \qquad \text{(Eq.5)} \qquad Abs_{CA} = (\text{Abs}_{Cracked} \text{ x } A_0) - \text{Abs}_{\text{non-cracked}} \text{ x } (A_0 - A_c) \qquad \text{(Eq.6)}$$

Table 6: Results of absorption coefficients of non-cracked area and crack area

		non-cracked area	Crack area
Aggregate	**w/c ratio**	**C_{abs} 10min (x10^{-6} m/min^{0,5})**	**C_{abs} 10min (x10^{-6} m/min^{0,5})**
A.N.	0,35	86	13 086
	0,55	143	18 648
Stalite	0,35	101	16 030
	0,55	203	21 753
Leca	0,35	123	17 457
	0,55	236	20 381

3.3 Oxygen permeability

Table 7 shows the results obtained for the oxygen permeability tests. These results include the oxygen permeability coefficients for non-cracked and cracked concrete specimens (K_{O2}), medium crack length (L_c) and the ratio between permeability coefficients in these two types of specimens. For the different mixtures studied, oxygen permeability coefficients were obtained between 13,9 e 205,6 x10^{-18} m^2.

Table 7: Oxygen permeability tests results

Aggregate	**w/c ratio**	**$K_{non\text{-}cracked,O2}$ (x10^{-18} m^2)**	**$K_{cracked,O2}$ (x10^{-18} m^2)**	**L_c (mm)**	**$K_{cracked,O2}$ / $K_{non\text{-}cracked,O2}$**
A.N.	0,35	13,9	14,4	9,0	1,04
	0,55	54,7	67,1	9,5	1,23
Stalite	0,35	15,4	16,9	14,5	1,10
	0,55	123,4	141,0	15,0	1,14
Leca	0,35	15,6	17,8	13,5	1,14
	0,55	188,7	205,6*	14,0	1,09

*Valid results were only obtained for 1 specimen

3.3.1 Oxygen permeability in non-cracked concrete

The analysis of the results shows that, oxygen permeability of concrete tends to increase with increasing w/c and increase of aggregate porosity. It was also possible to conclude that concretes produced with denser LWA, such as Stalite, lead to permeability values closer to those obtained in NWAC, even reaching equivalent performances when surrounded by high compact pastes (low w/c).

3.3.2 Oxygen permeability in cracked concrete

Regardless of the type of aggregate and w/c, it is confirmed that the concrete previously cracked had a higher permeability to O_2 than sane concrete. However, this increase was not very significant (less than 14%, in general). This is justified by the fact that only one crack has been inserted in the specimen and with a depth of less than 30% of its thickness. Since the specimens of different compositions were tested with different cracks lengths, it is not possible to establish a direct comparison between the different types of concrete. For mixtures with a w/c of 0.55, the increase in

permeability of cracked concrete was 23%, 14% and 9% for mixtures with NWA, Stalite and Leca, respectively. Although cracked NWAC have smaller cracks lengths, a greater increase of permeability in these concretes was verified than in LWAC. Thus, these results suggest that the introduction of cracks in LWAC has an impact on the gas permeability, which should be lower than in NWAC.

The obtained results did not allow to conclude on the influence of w/c in the increase of permeability, due to the introduction of cracking in concrete, for example in NWAC and LWAC with higher density, the increase of w/c led to a greater impact of cracking, but in the higher porosity LWAC an opposite trend was observed (Table 7, last column). Finally, it is possible to verify that the results suggest a smaller impact of cracking on LWAC with more porous aggregates, similar to what was observed for capillary absorption.

3.4 Carbonation resistance

The carbonation rate (K_c) ranged 16.5 to 25.9 mm/year^{0,5}, in non-cracked concrete specimens. In general, correlation coefficients (R^2) greater than 0.97 were obtained in the relation between the carbonation depth and the root of time. In Tables 8, 9 and 10 (Appendix) are presented the results obtained for the different types of specimens studied. For non-cracked specimens the values of (Kc) are presented; in the case of specimens with artificial cracks are presented values of Kc in the sane zone (non-cracked area), carbonation depths in the crack area ($Xc,_c$) and the cracks lengths for each test age; in the case of specimens with natural cracks the values of Kc in the sane and crack zone are presented.

3.4.1 Carbonation resistance in non-cracked concrete

The results show that LWAC with more porous aggregates (Leca) presented higher values of Kc than the other concretes produced with denser LWA (Stalite) or with NWA. For the mixture considered, with a w/c of 0,55, LWAC with Leca and Stalite presented Kc values around 13% and 57% higher than NWAC, respectively. This factor can be explained by the greater porosity of the LWA, which facilitate the diffusion of CO_2 into the concrete.

3.4.2 Carbonation resistance in cracked concrete

In the case of specimens with artificial cracks, the analysis of the influence of cracking on the carbonation resistance was complex, due to the fact that it was not possible to ensure that the artificial cracks presented similar values of L_c in the various specimens tested, for different compositions and different ages of exposure. For this reason, it was not possible to calculate $Kc,_{\text{cracked zone}}$, as in the case of natural cracks. In order to counter this phenomenon, it was necessary to define a new parameter that is independent of L_c, in order to allow a comparison between different mixtures based, the carbonation rate of the crack ($Kc,_C$). For the definition of this parameter, it was necessary to assume that carbonation rate after the length of the crack is similar to the carbonation rate of the sane zone (non-cracked concrete). Based on this hypothesis and using Eq.(2), it is possible to estimate the time affected to the progression of the carbonation front after the crack. For any of the exposure ages, the carbonation front exceeded the crack length, allowing the use of any of these values as the basis for the estimation of $Kc,_C$. However, it was decided to use the carbonation depth at 28 days, in order to minimize the effects of increased humidity inside the specimen. Thus, knowing the values of L_c, the sane zone carbonation rate ($Kc,_{\text{sane zone}}$) and the carbonation depth at 28 days ($Xc,_C$ 28d), the carbonation time after crack was determined, $t_{AC,}$ according to Eq.(7). Posteriorly, subtracting t_{AC} from the total test time (28 days), it is possible to estimate the time that the carbonation depth takes to travel the crack length, t_C. Finally, knowing t_C it is possible to determine the approximate value of $Kc,_C$ through equation Eq. (8). Table 11 shows the $Kc,_C$ values obtained for different mixtures and crack apertures studied, in Figure 1 are presented the relation between these two terms.

$$t_{AC} = \left(\frac{x_{c,28d} - L_c}{K_{c,sane\ zone}}\right)^2 \qquad \text{Eq.(7)}$$

$$K_{C,C} = \frac{L_c}{\sqrt{t_C}} \qquad \text{Eq.(8)}$$

As expected, the carbonation coefficient in the cracks, increased with the crack aperture. The largest increment in carbonation rate was observed between 0 (non-cracked) and 0.1mm crack apertures. From this value up to 0.3mm, the increment was proportionally lower.

Comparing the $Kc,_C$ values for crack aperture of 0.1mm, with the Kc values for non-cracked concrete, it is possible to verify that the crack influence tends to decrease with the increase of aggregate porosity. In this case, it can be concluded that the same cracking type has a greater impact on the NWAC carbonation rate than in LWAC. The relation between $Kc,_C$ and the aperture of artificial cracks considered for the different concretes is shown in Figure 1, results show the existence of a linear relationship between these two terms.

In the case of concrete with natural cracks, the analysis of the influence of cracking on the accelerated carbonation resistance was performed by a simpler process. On the one hand, the depth of carbonation at different ages was always lower than L_c, allowing the direct determination of the carbonation coefficient in the crack area, $Kc,_{crack\ zone}$. On the other hand, it was possible to ensure that the L_c of the different specimens tested at different exposure ages were the same. The direct comparison between the LWAC and LWAC with Leca is not valid, since the specimens had different crack apertures in the two types of concrete. However, it can be seen that, although the LWAC were produced with a crack aperture slightly smaller than the NWAC, the carbonation coefficient in the crack area was higher. This suggests a greater participation of the LWA in the natural cracks, contributing to the increase of $Kc,_{crack\ zone}$ in the LWAC when compared to the NWAC.

Table 11: Values obtained for $Kc,_C$

w/c	Aggregate	Crack aperture (mm)	$K_{c,C}$ (mm/year^{0,5})
0.55	NWA	0.1	38.9
		0.2	48.0
		0.3	58.8
	Stalite	0.1	41.7
		0.2	55.4
		0.3	65.2
	Leca	0.1	42.4
		0.2	53.0
		0.3	56.4

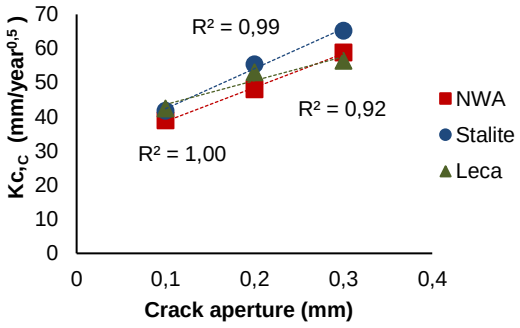

Figure 1: Relation between $Kc,_C$ and artificial crack aperture

3.5 Chloride penetration resistance

The diffusion coefficients (Dcl) varied between 8,9 and 37,1 x10^{-12} m^2/s in non-cracked concrete specimens. According to the classification proposed by Gjorv [20], it was possible to obtain mixtures with penetration of chlorides resistance of high to low level. Tables 12, 13 and 14 (Appendix) present the results obtained for the different types of specimens studied. In the case of non-cracked samples, the values referring to the mean values of the diffusion coefficients ($Dcl,_0$) are presented. For the cases of specimens with artificial and natural cracks, are presented the values referring to the diffusion coefficients in the non-cracked area ($Dcl,_{non\text{-}cracked\ area}$) and diffusion coefficients in the crack area ($Dcl,_{crack\ area}$).

3.5.1 Chloride penetration resistance in non-cracked concrete

By analyzing the results for non-cracked specimens, it can be seen that, in general, the chloride diffusion coefficient does not vary significantly with the type of aggregate, regardless of the w/c. This emphasizes the greater importance of paste quality compared to the type of aggregate in the resistance to penetration of chlorides of LWAC. However, it was observed that the participation of LWA in the diffusion of chlorides tends to be higher in concretes with more porous LWA surrounded by pastes of lower compactness.

3.5.2 Chloride penetration resistance in cracked concrete

As expected, the diffusion coefficient increased in cracked concrete, both in artificially cracked specimens and in natural cracked specimens. In concrete with artificial cracks, contrary to what was observed for the non-cracked specimens, the type of aggregate seems to have a greater influence on the diffusion of chlorides (Figure 2). Figure 3 shows the relation between diffusion coefficient of chlorides in the crack area and the aperture of artificial cracks in concrete with w/c of 0.35. In general, a linear growth of the diffusion coefficient with the crack aperture is confirmed, with correlation coefficients (R^2) higher than 0,95, similar to what was concluded in the case of carbonation resistance with artificial cracks. Taking into account the values of the diffusion coefficient in the sane area, it is concluded that the greatest diffusion increment occurs between 0 and 0.1 mm, becoming less relevant for higher values of crack aperture. Between 0.1 and 0.3 mm, there was an increase in the diffusion coefficient of on average only about 10% for each increment of 0.1 mm in crack aperture. Through the analysis of the test specimens with similar cracks lengths, it was possible to conclude that, unlike what has been observed in other properties studied in this work, the LWA seems to increase the cracking effect on the diffusion properties of the concrete.

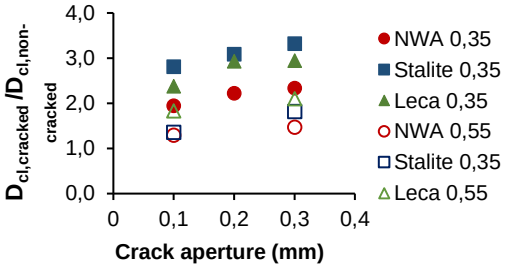

Figure 2: Relation between diffusion coefficient in crack area and non-cracked area

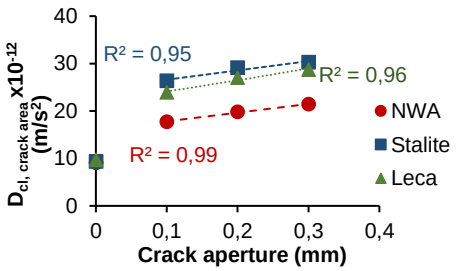

Figure 3: Relation between diffusion coefficient in crack area and respective crack aperture

In relation to concrete with natural cracks, similar to that observed for artificial cracks, the type of aggregate affected the diffusion of chlorides in the crack area. This phenomenon was slightly more important in concretes of lower w/c, where cracks may have increased more effectively the accessibility to LWA of greater porosity and diffusion. In this case, the greater participation of LWA in concrete with natural cracks is in agreement with the observed for the carbonation resistance.

4. Conclusion

The influence of cracks in the main transport properties and durability of LWAC and NWAC were studied. Based on the above experimental results, the following conclusions can be drawn:

- The obtained results allow us to conclude that, except for chloride diffusion, the influence of artificial cracks on durability was not significantly affected by the type of aggregate.
- It was observed that, for capillary absorption and oxygen permeability, cracked specimens tend to exhibit higher absorption and permeability over non-cracked reference specimens. However, the differences were not very significant.
- For carbonation and chloride penetration, a linear relationship between the diffusion properties and crack opening was found, taking into account artificial cracks between 0.1 and 0.3 mm.
- For carbonation and chloride penetration, crack aperture variation had greater relevance for cracks lower than 0.1 mm.
- For chloride penetration with artificial cracks between 0.1 and 0.3 mm, there was an increase in the diffusion coefficient of on average only about 10% for each increment of 0.1 mm in crack aperture.
- For concrete subjected to natural cracking, there was a greater participation of more porous aggregates, leading to a higher cracking influence on the LWAC durability.

Appendix

Table 8: Carbonation resistance results for non-cracked specimens

w/c	Aggregate	K_c (mm/year^{0,5})
0,55	NWA	16,5
	Stalite	18,6
	Leca	25,9

Table 9: Carbonation resistance results for specimens with artificial cracks

w/c	Aggregate	Crack aperture (mm)	$K_{c,non\text{-}cracked\ area}$ (mm/ano^{0,5})	Depth x_{cC} * (mm)			L_f * (mm)		
				28d	56d	91d	28d	56d	91d
0,55	NWA	0,1	16,3	11,6	14,0	14,2	10	10	11
		0,2	16,8	13,5	14,4	15,3	11	10	11
		0,3	16,3	15,3	16,0	13,5	12	11	9
	Stalite	0,1	18,2	12,3	15,3	16,1	10	12	10
		0,2	19,2	15,5	17,5	17,1	13	13	14
		0,3	18,8	19,3	16,9	18,3	16	14	14
	Leca	0,1	24,9	12,3	15,6	19,6	12	11	12
		0,2	24,8	15,4	17,9	22,4	15	17	15
		0,3	25,9	17,0	17,2	22,6	13	16	12

(*) Average of 2 results

Table 10: ***Carbonation resistance results for specimens with natural cracks***

w/c	Aggregate	Crack aperture (mm)	$K_{c,non\text{-}cracked\ area}$ (mm/year^{0,5})	$K_{c,crack\ area}$ (mm/year^{0,5})
0,55	NWA	0,15	18,0	50,0
	Leca	0,10	26,8	57,5

Table 12: Chloride penetration results for non-cracked specimens

Aggregate	w/c	$Dcl_{,0}$ x10^{-12} (m^2/s)
NWA	0,35	8,9
	0,55	16,3
Stalite	0,35	9,2
	0,55	17,3
Leca	0,35	9,7
	0,55	18,0

Table 13: Chloride penetration results for specimens with artificial cracks

Aggregate	w/c	Crack aperture (mm)	$D_{cl,non\text{-}cracked\ area}$ x10^{-12}(m^2/s)	$D_{cl,crak\ area}$ x10^{-12}(m^2/s)	L_f (mm)	$Dcl_{,crack}$ / $Dcl_{,non\text{-}cracked}$
NWA	0,35	0,1	9,1	17,7	9,0	1,9
		0,2	8,9	19,8	9,9	2,2
		0,3	9,2	21,4	12,6	2,3
	0,55	0,1	17,0	22,0	10,4	1,3
		0,3	16,5	24,2	9,8	1,5
Stalite	0,35	0,1	9,4	26,3	16,2	2,8
		0,2	9,4	29,1	16,0	3,1
		0,3	9,1	30,2	16,2	3,3
	0,55	0,1	16,4	22,2	11,2	1,4
		0,3	17,4	31,6	13,0	1,8
Leca	0,35	0,1	10,1	23,9	11,7	2,4
		0,2	9,2	27,0	11,5	2,9
		0,3	9,8	28,7	14,3	2,9
	0,55	0,1	17,8	32,5	11,1	1,8
		0,3	17,7	37,1	12,2	2,1

Table 14: Chloride penetration results for specimens with natural cracks

Aggregate	w/c	Crack aperture (mm)	$Dcl_{,non\text{-}cracked\ area}$ x10^{-12}(m^2/s)	$Dcl_{,crack\ area}$ x10^{-12}(m^2/s)	$Dcl_{,non\text{-}cracked}$ / $Dcl_{,crack}$
NWA	0,35	0,05	9,8	21,4	2,2
	0,55	0,05	18,8	26,9	1,4
		0,15	19,4	31,7	1,6
Leca	0,35	0,05	9,7	26,4	2,7
	0,55	0,05	19,6	34,2	1,8

5. References

[1] ACI224.1R-93, Causes, Evaluation and Repair of Cracks in Concrete Structures, ACI Committee 224, 1998.

[2] B. Gérard e J. Marchand, “Influence of cracking on the diffusion properties of cement-based materials, Part I: Influence of continuous cracks on the steady-state regime,” *Cement and Concrete Research,* vol. 30, pp. 37-43, 2000.

[3] G. D. Schutter, “Quantification of the influence of cracks in concrete structures on carbonation and chloride penetration,” *Magazine Concrete Research,* vol. 51, pp. 427-435, 1999.

[4] K. Wang, D. C. Jansen, S. P. Shah e A. F. karr, “Permeability study of cracked concrete,” *Cement and Concrete Research,* vol. 27, pp. 381-393, 1997.

[5] L. Sullivan-Green, Effect of crack width on carbonation: Implications for crack-dating, Thesis for the Degree of masters of science, field of Civil Engineering, Referido por Neves et al .(2010) ed., Evanston, Illinois: NORTHWESTERN UNIVERSITY, 2005.

[6] A. Djerbi, S. Bonnet, A. Khelidj e V. Baroghel-bouny, “Influence of traversing crack on chloride diffusion into concrete,” *Cement and Concrete Research,* vol. 38, pp. 877-883, 2008.

[7] C.-M. Aldea, S. P. Shah e A. Karr, “Effect of Cracking on Water and Chloride Permeability of Concrete,” *Journal of Materials in Civil Engineering,* vol. 11, nº 3, pp. 181-187, 1999.

[8] P. Zhang, F. H. Wittmann, T. Zhao e E. H. Lehmann, “Neutron imaging of water penetration into cracked steel reinforced concrete,” *Physica B: Condensed Matter,* vol. 405, nº 7, pp. 1866-1871, 2010.

[9] M. Ismail, A. Toumi, R. François e R. Gagné, “Effect of crack opening on the local diffusion of chloride in cracked mortar samples,” *Cement and Concrete Research,* vol. 38, nº 8-9, pp. 1106-1111, 2008.

[10] S. Y. Jang, B. S. Kim e B. H. Oh, “Effect of crack width on chloride diffusion coefficients of concrete by steady-state migration tests,” *Cement and Concrete,* vol. 41, pp. 9-19, 2011.

[11] Z. Yang, W. J. Weiss e J. Olek, “Water transport in concrete damaged by tensile loading and freeze-thaw cycling,” *Journal of Materials in Civil Engineering,* vol. 18, nº 3, pp. 424-434, 2006.

[12] S. Chandra e L. Berntsson, Lightweight Aggregate Concrete: Science, Technology, and Applications, USA: Noyes publications-Wiliam Andrew Publishing, 2003.

[13] J. Bogas e A. Gomes, “Non-steady-state accelerated chloride penetration resistance of structural lightweight aggregate concrete,” *Cement & Concrete Composites,* vol. 60, pp. 111-122, 2015.

[14] J. A. Bogas, B. Ferrer, J. Pontes e S. Real, “Biphasic Compressive Behavior of Structural Lightweight Concrete,” *ACI Materials Journal,* vol. 114, nº 1, pp. 49-56, 2017.

[15] J. A. Bogas, M. G. Gomes e S. Real , “Capillary absorption of structural lightweight aggregate concrete,” *Materials and Structures,* vol. 48, nº 9, pp. 2869-2883, 2014.

[16] S. Real e J. A. Bogas, “Oxygen permeability of structural lightweight aggregate concrete,” *Construction and Building Materials,* vol. 137, pp. 21-34, 2017.

[17] A. M. Vaysburd, “Durability of Lightweight Concrete Bridge In Severe Environments.,” *Concrete International,* vol. 18, nº 7, pp. 33-38, 1996.

[18] R. D. Browne, “Field investigations. Site & laboratory tests; maintenance, repair and rehabilitation of concrete structures – CEEC,” vol. Referido por Cortês (2014), 1991.

[19] O. Gjorv, “Performance and serviceability of concrete structures in the marine environment,” Symposium on Concrete for Marine tructures, CANMET/ACI. Ed. by P.K. Mehta,, 1996.

[20] J. A. Bogas, Caracterização de betões estruturais com agregados leves de argila expandida, Lisboa: Tese para obtenção do Grau de Doutor em engenharia civil. Universidade Técnica de Lisboa, Instituto Superior Técnico, 2011.

[21] E393, Betões – Determinação da absorção de água por capilaridade, Lisboa: Especificação LNEC, 1993.

[22] E392, Betões – Determinação da permeabilidade ao oxigénio, Lisboa: Especificação LNEC, 1993.

[23] E391, Betões – Determinação da resistência à carbonatação, Lisboa: Especificação Lnec, 1993.

[24] E463, Betões – Determinação do coeficiente de difusão dos cloretos por ensaio de migração em regime não estacionário, Lisboa: Especificação Lnec, 2004.

[25] NTBUILD492, Concrete, Mortar and Cement Based Repair Materials: Chloride Migration coefficient from Non-steady State Migration Experiments, Finland: Nordtest 492, 1999.

[26] J. A. Bogas e M. G. Gomes, “Estimation of water absorbed by expanding clay aggregates during structural lightweight concrete production,” *Materials and Structures,* vol. 45, nº 10, p. 1565–1576, 2012.